New Exact Solution of the One-Dimensional Schrödinger Equation and Its Application to Polarized Neutron Reflectometry

Huai Zhang and J. W. Lynn

Center for Superconductivity Research, Department of Physics, University of Maryland, College Park, Maryland 20742 and Reactor Radiation Division, National Institute of Standards and Technology, Gaithersburg, Maryland 20899

(Received 27 August 1992)

An analytic expression for the polarized neutron reflectivity $R^{\pm}(\theta,\lambda)$ from a superconductor with penetration depth λ is derived as an exact solution of the 1D Schrödinger equation in the continuum limit. The down-spin solution $R^{-}(\theta,\lambda)$ reveals a surprising oscillatory dependence on λ within a narrow angular range immediately above the total reflection angle, and in fact vanishes when λ and H satisfy certain conditions. This exact solution is applicable to other scattering problems with a general exponential dependence in the potential.

PACS numbers: 74.25.Ha, 03.65.Nk, 61.12.−q, 75.30.Pd

Polarized neutron reflectometry has developed in the last decade into a new technique to measure the magnetic field penetration depth λ in superconductors [1–5]. The merit of the method lies in the fact that it provides an absolute measurement of λ, and therefore neutron reflectometry has the capability in principle to make a model-independent determination of $\lambda(T)$. The technique has been successfully applied to Nb, Pb, and alloys, as well as to high-T_c systems. To interpret the reflectivity data, the scattering is calculated numerically from an "optical potential" theory, where the three-dimensional (3D) periodic nuclear scattering potential is approximated by an average nuclear potential of a continuum, and the magnetic field inside the superconductor is assumed to have the familiar (London and London [6]) exponential decrease with distance below the first critical field H_{c1}, $\mathbf{B}(x)=\mathbf{H}\exp(-x/\lambda)$. Since the values for H_{c1} are typically quite small, the magnetic interaction $-\boldsymbol{\mu}\cdot\mathbf{B}$ is usually much smaller than the nuclear interaction, and hence below T_c the ratio of the spin-dependent reflectivities R^{+}/R^{-} deviates significantly from unity only in the regime just above the critical angle θ_c for total reflection. This is just the regime where the continuum approximation works very well. We have found an analytic solution for $R^{\pm}(\theta,\lambda)$ for this problem that is valid throughout the entire angular range of interest. The down-spin solution $R^{-}(\theta,\lambda)$ in particular reveals a surprising oscillatory dependence on λ within a narrow angular range immediately above the total reflection angle, and in fact vanishes when λ and H satisfy certain conditions. This exact solution is applicable to other scattering problems with an exponential dependence in the potential, such as neutron reflectometry to determine the magnetization density profile at the surface of a ferromagnet [7].

We start with the 1D Schrödinger equation describing a neutron incident at angle θ on a plane-surfaced and semi-infinite superconducting sample placed in an applied magnetic field $\mathbf{H}$, and approximate the periodic arrangement of nuclei in the sample by a homogeneous continuum. This is a classic textbook 1D problem: To the incoming neutron the sample is represented as a simple potential barrier which consists of the neutron's nuclear interaction V_N with the average nuclear scattering potential and its magnetic interaction with the screening supercurrents in the sample. The change of the potential at the surface is then

$$V^{\pm}(x)=\left(\frac{2\pi\hbar^2}{m}\right)Nb\pm\boldsymbol{\mu}\cdot\mathbf{H}[\exp(-x/\lambda)-1]\,, \tag{1}$$

where the first term is V_N and the $\pm$ for the second (magnetic) term refers to incident neutrons with spin up or spin down. Here N is the number density and b is the coherent nuclear scattering amplitude. This is of course an idealized potential, where we neglect such processes as nuclear absorption, incoherent and phonon scattering, surface roughness, etc. When θ is small enough such that $\hbar^2k_x^2/2m$ is below this potential step the neutron is unable to overcome the barrier and therefore is totally reflected. The critical angle $\theta_c^{\pm}$ is defined when the two energies are equal, and when θ exceeds the critical angle then the neutron has a probability for both reflection and transmission. The reflectivity $R^{\pm}(\theta)$ depends of course on the details of the magnetic term in $V^{\pm}(x)$, particularly when θ is near the critical angle, and hence a measurement of $R^{\pm}$ can serve to determine the magnetic field penetration depth λ. We note that for thermal and cold neutrons θ_c is typically below 1°, and this is the conventional regime for neutron reflectometers [2,3,8], while for very cold neutrons θ_c can be much larger than 1°, and for ultracold neutrons $\theta_c\rightarrow 90°$ [9]. Our result applies to all these cases.

We define $u_N\equiv 4\pi Nb$ and $u_M\equiv\pm 2\mu Hm/\hbar^2$. Then Schrödinger's equation is

$$\frac{d^2\psi(x)}{dx^2}+[k_x^2-u(x)]\psi(x)=0\,, \tag{2}$$

with

$$u(x)=\begin{cases}0, & x<0\,,\\ u_N-u_M[1-\exp(-x/\lambda)], & x\geq 0\,,\end{cases} \tag{3}$$

where $k_x=k\sin(\theta)$ and $x\geq 0$ refers to the region inside

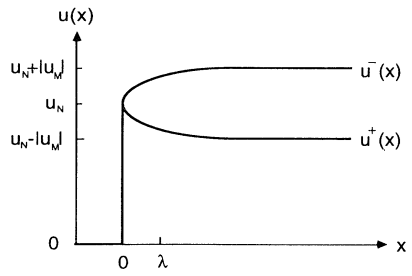

FIG. 1. Sketch of the interaction potential $u(x)$ for spin-up (+) neutrons and spin-down (−) neutrons. The subscripts N and M indicate nuclear and magnetic interactions, respectively. Note that u_N and $|u_M|$ have not been drawn to scale here, as $|u_M|$ is typically 2 orders of magnitude smaller than u_N.

the superconductor. Figure 1 shows a sketch of $u(x)$ for spin-up and spin-down neutrons. In the region $x \geq 0$ we define $\kappa \equiv +(k_x^2 - u_N + u_M)^{1/2}$, and letting $\psi(x) = \Phi(x) \times \exp(i\kappa x)$ and changing variables to $\xi = \lambda^2 u_M \exp(-x/\lambda)$, we obtain an equation for Φ:

$$\xi \frac{d^2\Phi}{d\xi^2} + (1 - 2i\kappa\lambda)\frac{d\Phi}{d\xi} - \Phi = 0 . \tag{4}$$

The expected asymptotic behavior that

$$\psi(x) \rightarrow C\exp(i\kappa x) \text{ as } x \rightarrow +\infty$$

imposes the boundary condition on Φ that $\Phi \rightarrow C$ as $\xi \rightarrow 0$, where C is a constant. We can now make a series expansion of Φ in ξ; we find that the solution to Eq. (4) is

$$\Phi = C\,{}_0F_1(1 - 2i\kappa\lambda;\xi) , \tag{5}$$

where ${}_0F_1$ is a generalized hypergeometric function defined by [10]

$${}_0F_1(\alpha;z) \equiv \sum_{n=0}^{+\infty} \frac{\Gamma(\alpha) z^n}{\Gamma(\alpha+n) n!} \tag{6}$$

for all z. We have that ${}_0F_1(\alpha;0) = 1$, which automatically gives the correct boundary condition for Φ as $x \rightarrow +\infty$. We note that ${}_0F_1(\alpha;z)$ with integer α is simply related to the Bessel function $J_{\alpha-1}$ for $z \leq 0$ and the modified Bessel function $I_{\alpha-1}$ for $z \geq 0$ via

$${}_0F_1(n;z) = \begin{cases} \dfrac{\Gamma(n) J_{n-1}(2|z|^{1/2})}{|z|^{(n-1)/2}} & \text{if } z \leq 0 , \quad (7a) \\ \dfrac{\Gamma(n) I_{n-1}(2z^{1/2})}{z^{(n-1)/2}} & \text{if } z \geq 0 . \quad (7b) \end{cases}$$

The solution of $\psi(x)$ in the $x \geq 0$ region is then

$$\psi(x) = C\,{}_0F_1(1 - 2i\kappa\lambda;\lambda^2 u_M \exp(-x/\lambda))\exp(i\kappa x) . \tag{8}$$

At $x = 0$, both $\psi(x)$ and $d\psi/dx$ must be continuous. Denoting r as the amplitude of the backscattered wave and normalizing the incoming wave to unity, we find that the solution for r is

$$r = \frac{(k_x - \kappa)\lambda(1 - 2i\kappa\lambda)\,{}_0F_1(1 - 2i\kappa\lambda;\lambda^2 u_M) - i\lambda^2 u_M\,{}_0F_1(2 - 2i\kappa\lambda;\lambda^2 u_M)}{(k_x + \kappa)\lambda(1 - 2i\kappa\lambda)\,{}_0F_1(1 - 2i\kappa\lambda;\lambda^2 u_M) + i\lambda^2 u_M\,{}_0F_1(2 - 2i\kappa\lambda;\lambda^2 u_M)} . \tag{9}$$

Hence the reflectivity $R = |r|^2$ is

$$R = \left| \frac{(k_x - \kappa)\lambda(1 - 2i\kappa\lambda)\,{}_0F_1(1 - 2i\kappa\lambda;\lambda^2 u_M) - i\lambda^2 u_M\,{}_0F_1(2 - 2i\kappa\lambda;\lambda^2 u_M)}{(k_x + \kappa)\lambda(1 - 2i\kappa\lambda)\,{}_0F_1(1 - 2i\kappa\lambda;\lambda^2 u_M) + i\lambda^2 u_M\,{}_0F_1(2 - 2i\kappa\lambda;\lambda^2 u_M)} \right|^2 . \tag{10}$$

We note that since $k_x = (2\pi/\lambda_n)\sin\theta$, where λ_n is the neutron's wavelength, the reflectivity R can be regarded as a function of λ_n for a fixed incident angle θ, or as a function of θ for a selected wavelength. The former is most appropriate for pulsed neutron sources while the latter is the practice at reactor-type neutron sources.

We take the case when the external magnetic field H is nonzero but below H_{c1} so that the sample is in its Meissner state; H is typically on the order of a few hundred oersteds or less. The region of total reflection ($R = 1$) becomes $k_x \leq (u_N - u_M)^{1/2}$. We have two different critical angles for spin-up (+) and spin-down (−) neutrons, respectively:

$$\theta_c^{\pm} \equiv \sin^{-1}[(u_N \mp |u_M|)^{1/2}\lambda_n/2\pi] . \tag{11}$$

Note that $\theta_c^- > \theta_c^+$. If we take typical values of $\lambda_n = 2.35$ Å, $H = 500$ Oe, and $u_N = 4.98\times10^{-5}$ Å^{-2} (appropriate for niobium), the critical angles are $\theta_c^+ = 0.1489°$ and $\theta_c^- = 0.1533°$, and the critical angle splitting is $\theta_c^- - \theta_c^+ = 0.0044°$.

Figure 2 shows $R^+(\theta)$ (dash-dotted curve) and $R^-(\theta)$ (solid curve) for three different choices of the penetration depth λ: (a) 400 Å, (b) 1000 Å, and (c) 1600 Å, with $\lambda_n = 2.35$ Å, $H = 500$ Oe, and $u_N = 4.98\times10^{-5}$ Å^{-2}. The dash-double-dotted line is the reflectivity for $H = 0$ (nuclear potential only). First consider the curves for $R^+(\theta)$. As θ exceeds θ_c^+, $R^+(\theta)$ decreases monotonically, and the larger λ is, the slower $R^+(\theta)$ decreases above θ_c^+. This is the type of behavior expected based on previous (numerical) results. The behavior of $R^-(\theta)$, on the other hand, is surprising, as it does not always decrease monotonically as a function of θ above θ_c^-. For example, at $\lambda = 1000$ Å, $R^-(\theta)$ almost dips to zero immediately above θ_c^- [Fig. 2(b)]. Beyond this dip, $R^-(\theta)$ is slightly above $R^+(\theta)$, reflecting the fact that the asymptotic value of $u^-(x)$ is above $u^+(x)$ by $2|u_M|$ (Fig. 1). As θ continues to increase, $R^-(\theta)$ and $R^+(\theta)$ merge into one curve as $2|u_M|$ becomes small compared to the kinetic energy term controlled by k_x

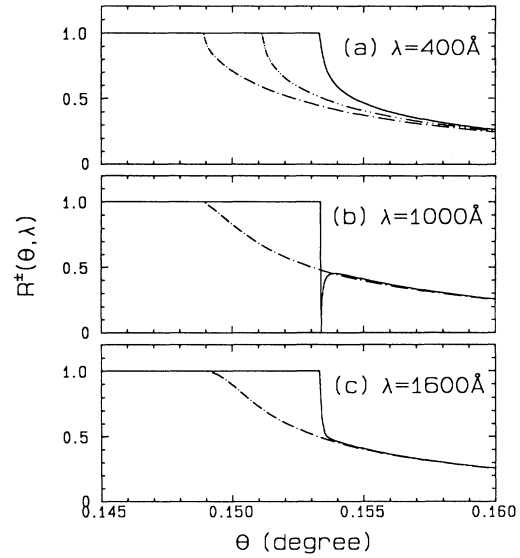

FIG. 2. Reflectivity calculated from Eq. (10) for spin-up $[R^+(\theta,\lambda)$ (dash-dotted curves)] and spin-down $[R^-(\theta,\lambda)$ (solid curves)] neutrons, as a function of θ, for three different values of the magnetic penetration depth λ. Parameters used for plotting are $\lambda_n=2.35$ Å, $H=500$ Oe, and $\mu_N=4.98\times10^{-5}$ Å^{-2} (for niobium). (a) $\lambda=400$ Å, (b) 1000 Å, and (c) 1600 Å. The dash-double-dotted line in (a) is the reflectivity of $H=0$.

$=k\sin\theta$. Thus these spin-dependent effects are most discernible in the vicinity of the critical angles.

The "dip" in the reflectivity profile for spin-down neutrons shown in Fig. 2(b) was an unexpected feature revealed by the analytic expression for $R(\theta,\lambda)$. In actual reflectivity measurements from thin films we typically see oscillatory behavior in $R(\theta)$ due to interference from the waves scattered from the front and back surfaces of the sample. In the present case, however, the sample is assumed to be infinitely thick and hence this structure in $R^-(\theta)$ must have a different nature. This λ-dependent resonance effect is worth studying because it has the potential to be developed into a sensitive way to measure λ.

To study the anomalous resonant transmission analytically, let us consider Eq. (10) in the κ range where $0<\kappa\lambda\ll1$. For the magnetic field range we are considering and for most materials this guarantees that $0<\kappa/k_{xc}\ll1$, where $k_{xc}\equiv(u_N-u_M)^{1/2}$. We therefore expand both the numerator and the denominator of r in Eq. (9) to first order in $\kappa\lambda$ and κ/k_{xc}, and write r as

$$r\cong\frac{(f_1+if_2)-(f_3+if_4)\kappa\lambda}{(f_1-if_2)+(f_3-if_4)\kappa\lambda}, \tag{12}$$

where f_1, f_2, f_3, and f_4 are real functions defined by

$$f_1\equiv k_{xc}\lambda\,{}_0F_1(1;\lambda^2u_M),\quad f_2\equiv-\lambda^2u_M\,{}_0F_1(2;\lambda^2u_M),$$

$$f_3\equiv{}_0F_1(1;\lambda^2u_M)+2\lambda^2u_M\,{}_0F'_{1,1}(2;\lambda^2u_M),$$

and

$$f_4\equiv2k_{xc}\lambda[{}_0F_1(1;\lambda^2u_M)+{}_0F'_{1,1}(1;\lambda^2u_M)],$$

where ${}_0F'_{1,1}$ denotes the first derivative of ${}_0F_1$ with respect to its first variable. These four dimensionless functions are independent of θ and the neutron wavelength λ_n. Rather, they are determined only by the shape and magnitude of the potential through parameters such as u_N, u_M, and λ. We remark that since the ${}_0F_1(\alpha;z)$ with integer α are simply related to Bessel functions [Eq. (7)], and noting that $J_n(z)$ is oscillatory while $I_n(z)$ is monotonic, we may anticipate an oscillatory dependence of r on λ for spin-down neutrons ($u_M<0$).

In this κ range the reflectivity becomes

$$R\cong\frac{(f_1-f_3\kappa\lambda)^2+(f_2-f_4\kappa\lambda)^2}{(f_1+f_3\kappa\lambda)^2+(f_2+f_4\kappa\lambda)^2}. \tag{13}$$

Hence a sufficient condition for a total transmission to occur is given by simultaneously satisfying $f_1=f_3\kappa\lambda$ and $f_2=f_4\kappa\lambda$. Eliminating $\kappa\lambda$ we find

$$0<\frac{f_1}{f_3}=\frac{f_2}{f_4}\ll1. \tag{14}$$

This functional dependence means that it is the *shape* of the potential curve that determines whether this total transmission may occur, independent of the wave vector k_x or angle θ. The value of k_x (and θ) at which this total transmission will occur can be calculated by using $\kappa\lambda=f_1/f_3$. An approximate expression for Eq. (14) can be obtained by noting that the solutions are close to $f_1\cong0$, which means ${}_0F_1(1;\lambda^2u_M)\cong0$. Hence the condition for the total transmission (of the down-spin state) becomes $J_0(2\lambda(2\mu Hm/\hbar^2)^{1/2})\cong0$, so that to a good approximation $2\lambda(2\mu Hm/\hbar^2)^{1/2}$ needs to be a root of the zeroth-order Bessel function. Solutions to any accuracy may be obtained by graphically solving Eq. (14). We emphasize that here it is the shape of the potential curve that determines whether this total transmission may occur. In contrast to the *k_x-oscillatory type* of resonant transmission, we refer to the anomalous transmission discussed above as the *potential-profile-dependent and single-dip* type. Both have the same physical origin—the reflected waves add up destructively. Indeed we have found a similar anomalous transmission in a very simple two-step potential profile.

The angular difference between the total transmission angle θ_{tt} and the critical angle θ_c^- can be calculated from

$$k_{x_{tt}}^2-k_{xc}^2=(f_1/f_3\lambda)^2. \tag{15}$$

When the total transmission condition [Eq. (14)] is met, f_1/f_3 is much smaller than 1, and therefore the right-hand side of Eq. (15) is very small and θ_{tt} is very close to θ_c^-. Then Eq. (15) can be rewritten as

$$\sin\theta_{tt}-\sin\theta_c^-=\frac{\lambda_n}{4\pi k_{xc}}\left[\frac{f_1}{f_3\lambda}\right]^2, \tag{16}$$

where we note that the right-hand side is proportional

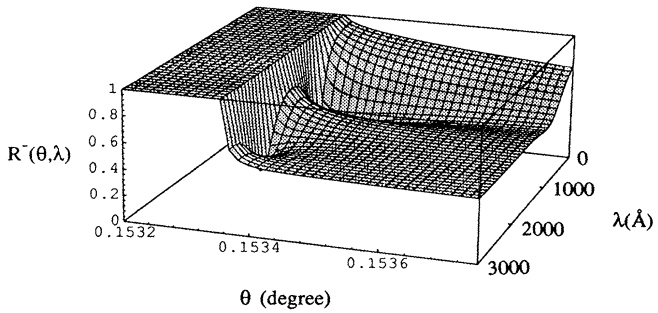

FIG. 3. Reflectivity $R^{-}(\theta,\lambda)$ calculated from Eq. (10) for spin-down neutrons, plotted as a function of both variables θ and λ. Parameters λ_n, H, and u_N used are the same as those in Fig. 2. The oscillatory dependence of $R^{-}(\theta,\lambda)$ on λ can be clearly seen.

to the neutron wavelength. Taking $H=500$ Oe, $u_N=4.98\times10^{-5}$ Å^{-2}, and $\lambda\cong1002$ Å where the first total transmission occurs, we have $f_1/f_3\simeq0.0545$ and $k_{xc}=(u_N+|u_M|)^{1/2}=0.00715$ Å^{-1}, which gives $\sin\theta_{tt}-\sin\theta_c^{-}=3.3\times10^{-8}\lambda_n$, or $\theta_{tt}-\theta_c^{-}=(2\times10^{-6}/\cos\theta_c^{-})\lambda_n$ where the angles are in degrees. Only in the very cold to ultracold neutron regime will this angular difference be possible to resolve experimentally with present instrumentation. The resonance condition may be tuned by varying the magnetic penetration depth (with temperature) or by varying the applied field.

Since the condition on the occurrence of the total transmission depends on an oscillatory Bessel function, the λ dependence of $R^{-}(\theta,\lambda)$ for $\theta\gtrsim\theta_c^{-}$ must also be quasiperiodic. Figure 3 is a 3D plot of $R^{-}(\theta,\lambda)$ of Eq. (10) as a function of θ and λ to show its oscillatory dependence on λ. The parameters λ_n, H, and u_N are the same as those used in Fig. 2.

We have focused our discussions on neutron reflectometry measurements of the magnetic penetration depth λ in superconductors, as this was the problem which led us to this investigation. However, these results are not restricted to neutron scattering; the exact solution [11] for $R^{\pm}(\theta,\lambda)$ can be applied to other scattering problems where the scattering potential has an exponential dependence with distance. Another example for neutrons is the problem of the magnetization at the surface of a ferromagnet, where the magnetization in the surface layer is expected to deviate from the bulk by [7] $\Delta\mu(z)=\Delta\mu_s\exp(-z/\xi)$, where ξ is the magnetic coherence length, and both $\Delta\mu_s$ and ξ are temperature dependent. Our solution can be immediately applied to this system, with ξ replacing λ. Indeed polarized neutron reflectometry has been shown to be a sensitive probe to determine the temperature dependence of the magnetization at the surface of ferromagnets.

We would like to thank R. A. Ferrell, C. J. Lobb, C. F. Majkrzak, and S. K. Satija for helpful conversations. The research at Maryland is supported by the NSF, DMR 89-21878.

[1] G. P. Felcher, R. T. Kampwirth, K. E. Gray, and Roberto Felici, Phys. Rev. Lett. **52**, 1539 (1984).
[2] G. P. Felcher, Roberto Felici, R. T. Kampwirth, and K. E. Gray, J. Appl. Phys. **57**, 3789 (1985).
[3] R. Felici, J. Penfold, R. C. Ward, E. Olsi, and C. Matacotta, Nature (London) **329**, 523 (1987).
[4] A. Mansour, R. O. Hilleke, G. P. Felcher, R. B. Laibowitz, P. Chaudhari, and S. S. P. Parkin, Physica (Amsterdam) **156 & 157B**, 867 (1989).
[5] K. E. Gray, G. P. Felcher, R. T. Kampwirth, and R. Hilleke, Phys. Rev. B **42**, 3971 (1990).
[6] F. London and H. London, Proc. R. Soc. London A **149**, 71 (1935); Physica (Utrecht) **2**, 341 (1935).
[7] T. Wolfram and R. E. De Wames, *Progress in Surface Science* (Pergamon, Oxford, 1975), Vol. 2, p. 233; G. P. Felcher, Phys. Rev. B **24**, 1595 (1981).
[8] C. F. Majkrzak, Physica (Amsterdam) **173B**, 75 (1991).
[9] R. Golub, D. Richardson, and S. K. Lamoreaux, *Ultra-Cold Neutrons* (Adam Hilger, Bristol, 1991).
[10] Bateman Manuscript Project, *Higher Transcendental Functions* (McGraw-Hill, New York, 1953), Chap. 4.
[11] For a review of other exact solutions related to reflection measurements see, for example, J. Lekner, *Theory of Reflection of Electromagnetic and Particle Waves* (Nijhoff, Dordrecht, 1987), Chap. 2.